

Anisotropy in mechanical properties of forged isotactic polypropylene

Satoshi Osawa*

Department of Materials Science and Technology, Science University of Tokyo,
Yamaguchi College, Onoda, Yamaguchi 756 Japan

and Roger S. Porter

Polymer Science and Engineering Department, University of Massachusetts, Amherst,
MA 01003, USA

(Received 8 May 1995; revised 24 July 1995)

The anisotropy in mechanical properties of forged isotactic polypropylene (iPP) has been investigated by microhardness indentation and Izod impact tests. The results are important, since the major changes in these properties that have been found can influence the growing number of applications where iPP is indented or impacted in use. The iPP had a molecular weight of 2.9×10^5 and an initial fraction of 64% α -crystal. For these samples forged at 140°C (resulting in α -crystal only plus amorphous), the indentation hardness perpendicular to the plane direction, $H(\perp)$, slightly increased with draw. The hardness tested parallel to the film surface, $H(\parallel)$, decreased rapidly with draw. For the sample forged at 50°C (containing draw-generated smectic), both $H(\parallel)$ and $H(\perp)$ decreased with draw, suggesting the softness of the smectic phase. The anisotropy, $H(\perp)/H(\parallel)$, for samples forged at 50°C is higher than that for samples forged at 140°C at a comparable compression ratio (CR), e.g. at $CR = 7.5$, $H(\perp)/H(\parallel)$ for 50°C and 140°C are 2.7 and 2, respectively. The impact strength of forged iPP was very different from the results of the indentation test. For samples forged at 50 and 140°C, the strength both parallel and perpendicular to the forged sample surface increased strongly with draw. The strength tested along the planar direction is about twice that tested through the thickness direction. Testing in each direction broke the samples into layers. The mechanism of energy absorption is closely related to the morphology-developed planar orientation with the crystal b -axis orientation normal to the plane direction. Copyright © 1996 Elsevier Science Ltd.

(Keywords: mechanical properties; isotactic polypropylene; anisotropy)

INTRODUCTION

It has been well recognized that the anisotropy in mechanical properties of oriented polymer materials arises from the anisotropic morphology^{1–3}. Considerable attention has been focused on the anisotropic mechanical property in the machine (MD) and transverse directions (TD) of unidirectionally oriented polymers. On planar deformation, on the other hand, the enhancement of balanced mechanical properties in the plane direction have been achieved^{4–12}. The maximum increase of the tensile modulus in the plane direction is about three-eighths that for uniaxially drawn films¹⁰ and about four times higher than the modulus of uniaxially oriented films in the transverse direction. For isotactic polypropylene (iPP) the directional dependent properties reported here indicate that both indentation and impact properties are changed markedly by high planar draw. Another practical consequence for iPP draw is the enhancement of optical clarity through the thickness^{13,14}. The anisotropy of planar oriented polymer is between the thickness direction, i.e. normal direction (ND) and the MD (or TD) direction.

Recently, a remarkable enhancement of impact properties of planar oriented iPP has been observed through the thickness (ND). Under certain conditions, the impact toughness of biaxially rolled polypropylene is over 30 times that of the undrawn material¹⁵. The Bethlehem Steel process can make 2.4×2.4 biaxially oriented iPP sufficiently tough to stop a 35 mm bullet¹⁶. Bonded cross-laminates of uniaxially drawn iPP have also exhibited improved impact toughness and ballistic energy absorption¹⁷. It is noted that the increase in the property through the ND is much higher than that along MD (or TD). This is related to the anisotropic morphology between the ND and the plane direction. Among the many valuable studies of processing, structure and properties of planar or biaxially oriented iPP, the correlation between the anisotropic morphology and the anisotropic mechanical properties related to ND is not well established. It may be because of the difficulty in evaluating the mechanical properties from the thickness.

We have shown that deformation of the common iPP morphology of spherulites by forging results in a layer structure parallel to the plane¹⁴. Further, the initial α -crystals transform to the smectic form with the b -axis orientation normal to the planar direction. To identify the relation of such structural anisotropy to properties, it is necessary to evaluate the properties for directions both

* To whom correspondence should be addressed. Present address: Kamazawa Institute of Technology, Nonouchi, Ishikawa 921, Japan

parallel and perpendicular to the plane. Microhardness tests¹⁸⁻²¹ are available to evaluate mechanical properties through the thickness. It is possible to test small sample areas. Balta Calleja *et al.*¹⁹ developed indentation hardness tests for the investigation of the microstructure of semicrystalline polymers of various morphological forms. In this study of forged iPP, the microhardness indentation and Izod impact tests have been carried out through the film thickness and in the planar directions. The results of indentation and impact tests are compared with the anisotropic morphology.

EXPERIMENTAL

The isotactic polypropylene (iPP) for study (supplied by Phillips Co.) had a melt index of 4.0 corresponding to a molecular weight, M_w , of 2.9×10^5 . The original pellets were moulded into 5.6 mm thick sheet in a vacuum press at 220°C. The mould was quenched by ice water. The original sheet had a heat of melting of 87.9 J g^{-1} , corresponding to 64% weight fraction crystallinity when 138.1 J g^{-1} was used for the perfect crystal²² (the volume fraction crystallinity was 61%). The moulded sheets were uniaxially compressed under isothermal conditions, at temperatures of 50 and 140°C, by using a dynamic test system composed of an Instron model 1333 which allows on-line measurement of load and displacement during the deformation process. The forging experiment consists of squeezing the polymer out of the compression zone. The compression area (25.4 mm diameter cylinder) remains unchanged during forging. The compression draw ratio, CR , is defined by the sample thickness before (d_0) and after (d) compression, i.e. $CR = d_0/d$. The range prepared in this study is up to $CR = 36$ (6×6). A detailed description of the method has been given^{23,24}.

Microhardness was measured at room temperature using a hardness tester (Akashi AKVII). The hardness value was derived from the residual projected area of indentation according to $H = KP/d^2$, d being the length of the impression diagonal, P the contact load applied and K a factor of 1.854. The load cycle and load were 25 s and 1 kg, respectively. Izod impact strength of unnotched samples was measured by an Izod impact tester (Custom Scientific Instruments Inc., model CS-183TI-061). The tests were performed at room temperature for three mutually perpendicular directions of the sample.

RESULTS AND DISCUSSION

The mechanical field of uniaxial compression (forging) leads to an equibiaxial deformation, which results in a planar texture²⁵. The samples forged at 50°C result in a smectic phase^{23,24}. No smectic phase is observed in the sample forged at 140°C (only α -crystals). Previous X-ray studies of the forged iPP^{26,27} have shown two types of crystal textures, referred to as common planar orientation and crystal b -axis orientation, along a normal direction to the sample surface, i.e. $(0k0)$ is parallel to the planar direction. The $(0k0)$ is the main slip plane on the forging of iPP²⁶. A schematic drawing of the two types of crystal orientation are shown in Figure 1. The planar orientation and the b -axis orientation correspond to A and B, respectively. The relative amount of B-type texture is higher if iPP is deformed via the order-

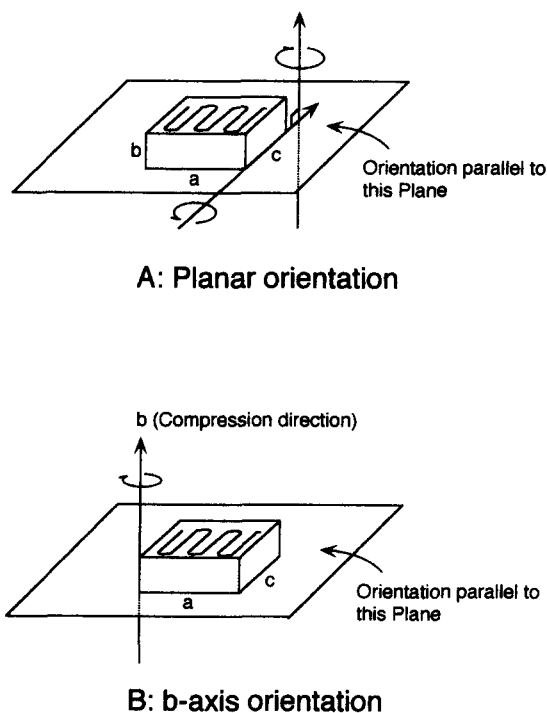


Figure 1 Schematic of crystal orientations. (A) Planar orientation (c -axis is lying in the plane, a and b -axes are random around the c -axis). (B) The b -axis is perpendicular to the plane direction, a - and c -axes are random around the b -axis

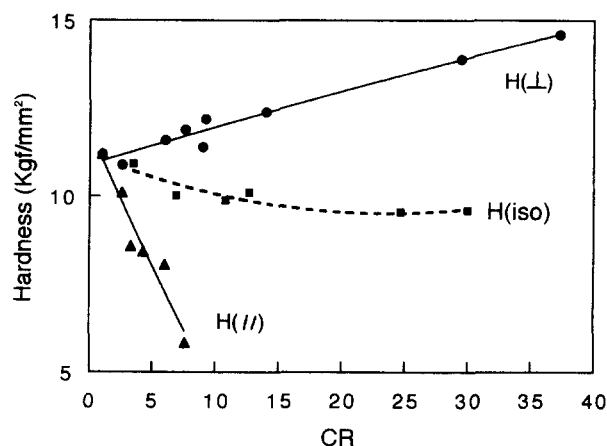


Figure 2 The microhardness of the sample forged at 140°C as a function of CR for perpendicular, $H(\perp)$, and parallel, $H(\parallel)$, to the plane direction

disorder process (in this case, smectic phase is generated during the deformation at 50°C), rather than by deformation at 140°C (ref. 26). For both cases A and B, the c -axis is lying in the plane direction (film surface direction).

Microhardness

Figure 2 shows the microhardness measured by indentation for the sample forged at 140°C (it consists of α -crystal only plus amorphous). The geometry of the indentation test is indicated in Figure 3. The hardness tested perpendicular to the film surface, $H(\perp)$, increases slightly with compression draw ratio (CR). On the other

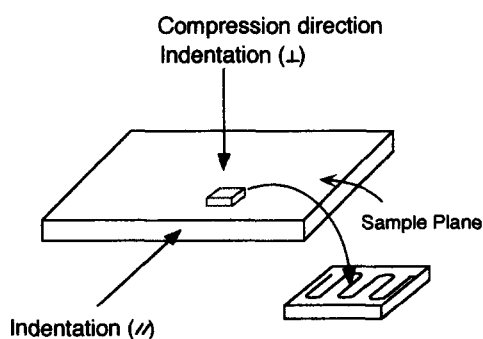


Figure 3 Schematic of the sample geometry for the indentation test for microhardness

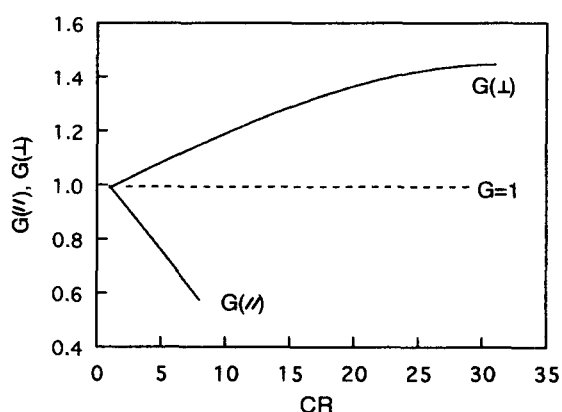


Figure 4 The normalized orientation effects of draw on microhardness for perpendicular, $G(\perp)$, and parallel, $G(\parallel)$, to the plane direction as a function of CR

hand, the value tested parallel to the film surface, $H(\parallel)$, decreases rapidly with draw. Above $CR = 10$, it is difficult to measure $H(\parallel)$ because the sample is so fragile in this direction that cracks develop along the film surface direction (along $0k0$). Thus, the sample breaks easily from the edge.

Polymer hardness is known to be influenced by crystallinity¹⁹. According to our previous study²⁸, the crystallinity decreases with compression draw. Therefore, $H(\parallel)$ and $H(\perp)$ in Figure 2 include the effects of crystallinity in addition to the orientation effects. Balta Calleja and coworkers reported¹⁹ that polymers can display a lamellar morphology of stiff flat crystals intercalated by amorphous compliant layers. The overall microhardness, H , can be described by a simple binary additive model for an isotropic sample:

$$H = wcH_c + (1 - wc)H_a \quad (1)$$

where H_c and H_a are the hardness of crystalline and amorphous components, respectively, and wc is the volume fraction of the crystalline phase. The H and wc of the undrawn original sample in this study were 9.36 kgf mm^{-2} and 0.61 , respectively. Taking H_a of 3.06 kgf mm^{-2} (ref. 19), H_c is estimated to be 13.4 kgf mm^{-2} . This approaches the value reported by Balta Calleja *et al.*¹⁹ (14.5 kg mm^{-2}). If the iPP sample in Figure 2 is isotropic, i.e. there is no planar orientation effect on hardness, the overall hardness (H) obeys the dotted line as calculated by equation (1). The wc is calculated from the weight fraction crystallinity, X_c , and sample densities, ρ , of our

previous study of forged iPP²⁸, i.e. $wc = X_c(\rho/\rho_c)$, where $\rho_c = 0.936 \text{ g cm}^{-3}$ is the density of α -crystals²⁹. The dotted line is expressed by a curve fitted to the line of $H(\text{iso})$. When the hardness data for directions parallel and perpendicular to the film plane are expressed by curve-fitted formulae of $H(\parallel)$ and $H(\perp)$, respectively, the mean effects of orientation with compression draw can be normalized by functions of $G(\parallel) = H(\parallel)/H(\text{iso})$ and $G(\perp) = H(\perp)/H(\text{iso})$. The $G(\parallel)$ and $G(\perp)$ are plotted in Figure 4. Here $G = 1$ is for no orientation. It is clear that the mean effect of orientation on hardness for the parallel direction is greater than that for the perpendicular.

Figure 5 shows the microhardness of iPP forged at 50°C for parallel, $H(\parallel)$ and perpendicular, $H(\perp)$, to the plane direction. These samples are composed of α -crystal, smectic and amorphous phases. It is noted that both $H(\parallel)$ and $H(\perp)$ decrease with compression draw, although the anisotropy $H(\perp)/H(\parallel)$ is higher than that for samples without the smectic phase (forged at 140°C), e.g. at a comparable CR of 7.5, $H(\perp)/H(\parallel)$ of samples forged at 50°C and 140°C are about 2.7 and 2, respectively. The α -crystal transforms to smectic as CR is increased. Therefore, the results in Figure 5 suggest

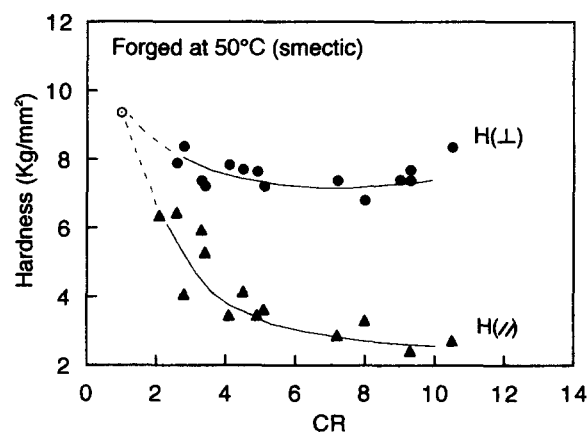


Figure 5 The microhardness of the sample prepared at 50°C as a function of CR for perpendicular, $H(\perp)$, and parallel, $H(\parallel)$, to the plane direction

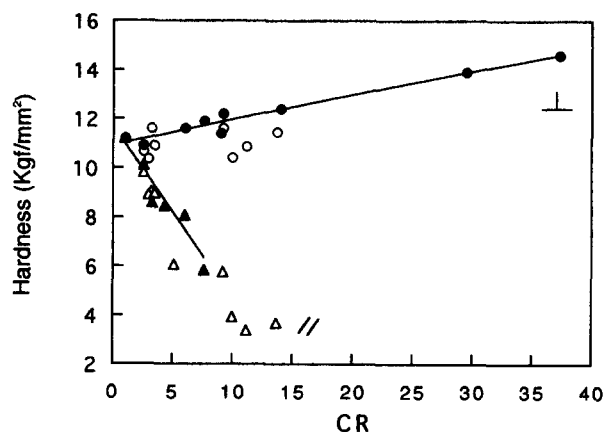


Figure 6 The microhardness of subsequently heat-treated (140°C for 30 min) samples forged at 50°C for perpendicular (\circ) and parallel (Δ) to the plane direction with the data of iPP forged at 140°C for perpendicular (\bullet) and parallel (\blacktriangle) to the plane direction in Figure 2

that smectic is a soft phase. This smectic phase completely reverts back to α -crystals by heat treatment at 140°C. Figure 6 shows $H(\parallel)$ and $H(\perp)$ of the subsequently heat-treated (140°C for 30 min) samples forged at 50°C with the data of Figure 2 (for samples forged at 140°C). Each $H(\parallel)$ and $H(\perp)$ roughly follows on lines expressed by functions $H(\parallel)$ and $H(\perp)$ in Figure 2. This result confirms that the decrease in $H(\parallel)$ and $H(\perp)$ for iPP forged at 50°C is due to the generation of the soft smectic phase. In Figure 6, the anisotropy, $H(\perp)/H(\parallel)$, in both the subsequently heat-treated sample (forged at 50°C) and the sample forged at 140°C is comparable, whereas, $H(\perp)/H(\parallel)$ of the smectic-containing sample (forged at 50°C) is higher than that for samples without the smectic (forged at 140°C). These results suggest that the anisotropy of microhardness in the smectic phase is higher than that in the α -crystal phase at a comparable CR. The draw-generated smectic phase is a laterally (for the direction perpendicular to the molecular axis) disordered form of α -crystal²³. The fraction of smectic increases with draw²⁸. Further, the *b*-axis orientation normal to the planar direction (i.e. the disordered main slip plane of 0*k*0 lying parallel to the planar direction) becomes prominent²⁶. These structural changes with draw lower $H(\parallel)$ rather than $H(\perp)$ of the smectic, resulting in a higher anisotropy, $H(\perp)/H(\parallel)$, of the smectic phase.

Impact strength

The impact strength of forged iPP is very different from the results of indentation tests. The sample geometry for the measurements in all three orthogonal directions is shown in Figure 7 with definition of direction. The unnotched samples were tightly clamped, so that the samples break at the edge of the hammer,

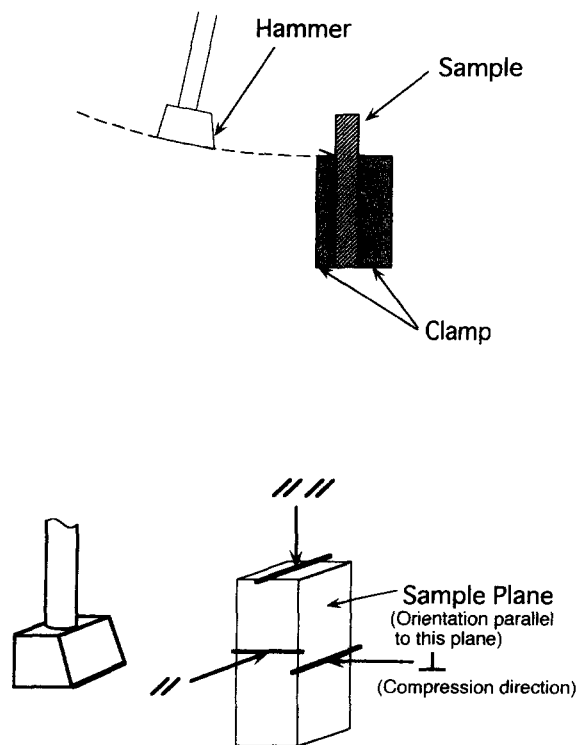


Figure 7 Schematic of sample geometry for Izod impact test

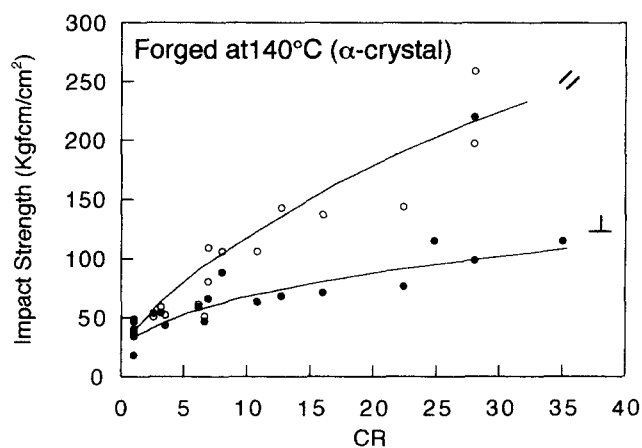


Figure 8 The impact strength of the sample prepared at 140°C (α -crystal) tested parallel (○) and perpendicular (●) to the plane direction

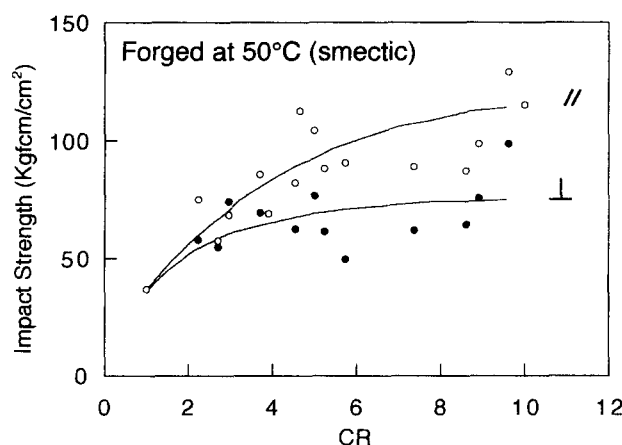


Figure 9 The impact strength of the sample prepared at 50°C (with smectic) tested parallel (○) and perpendicular (●) to the plane direction

marked by a thick line. Figure 8 shows the impact strength of the sample forged at 140°C (α -crystal only plus amorphous) for the parallel (\parallel) and perpendicular (\perp) directions. For both directions, the strength increased with compression draw. Further, the value of (\parallel) is about twice that of (\perp) at a comparable CR. For the direction (\parallel) (see Figure 7) only the sample of CR < 2.6 could be measured, since the sample thickness for higher CR is insufficient to clamp the sample. Even for such a low CR of 2.6, the value for (\parallel) drops to 4 kgfcm cm⁻² (about one tenth of that for original undeformed iPP). This drop is due to the planar orientation of molecular chains (type A in Figure 1) and *b*-axis orientation (type B in Figure 1) normal to the (\parallel) direction, i.e. the (0*k*0) plane is parallel to the planar direction. The (0*k*0) is the main slip plane on the forging of iPP²⁶. The impact strength of (\parallel) and (\perp) at CR = 30 are about seven and three times that of the original unoriented sample, respectively. The results contrast with the results of indentation hardness for which the draw effects are minor for (\perp) (only 1.3 times increase at CR = 30) or the (\parallel) decrease with draw. Figure 9 shows the impact strength of samples containing smectic phase (forged at 50°C). Both (\parallel) and (\perp) increase with draw. The strength is about 10% higher than that of samples containing only α -crystal in contrast to the

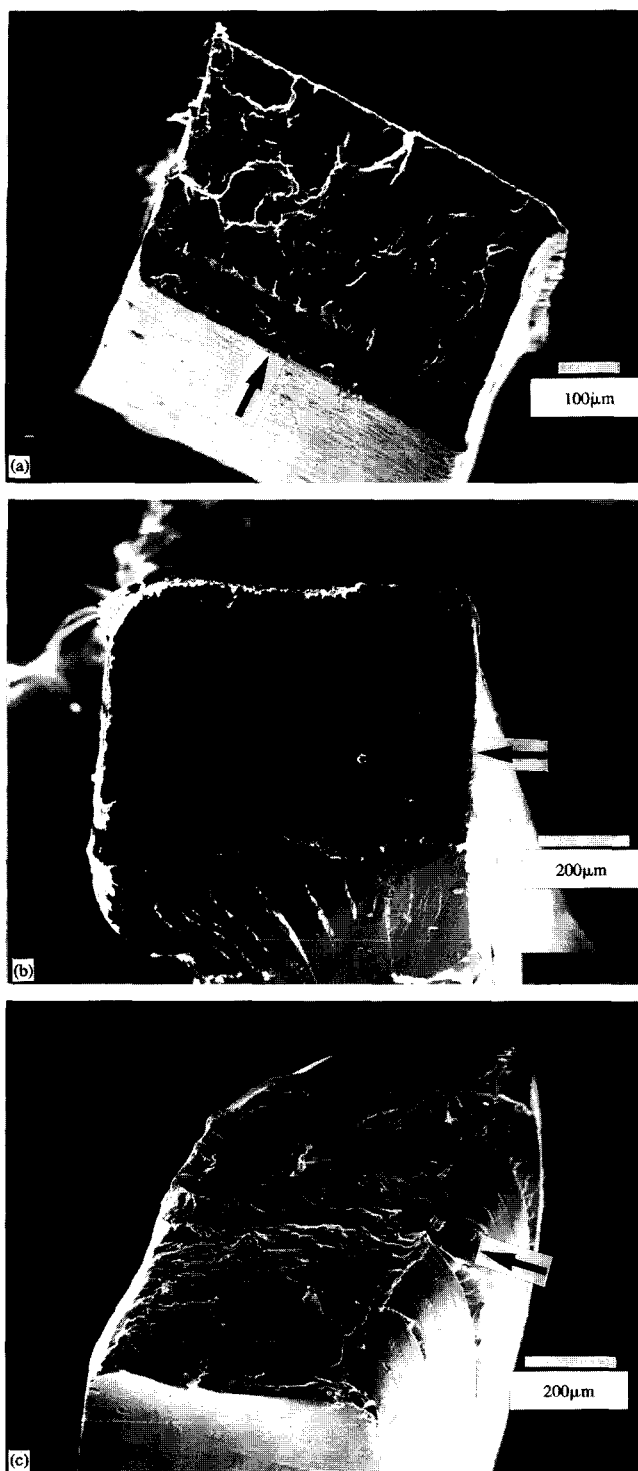


Figure 10 The SEM photographs of the fractured surface of the sample after Izod impact tests. (a) Original sample (undrawn). (b) Prepared at 140°C and $CR = 8$ for the test of (\perp). (c) Same sample as in (b) for the test of (\parallel). The arrows indicate the direction in which the hammer went through the sample

indentation tests for which the hardness decreases by the generation of smectic phase.

In our previous study¹⁴, forged iPP fractured by delamination into a layered structure on tensile tests. This feature was most prominent for highly compressed samples. Further, the layer structure was seen to be composed of a stacking of deformed spherulite planes

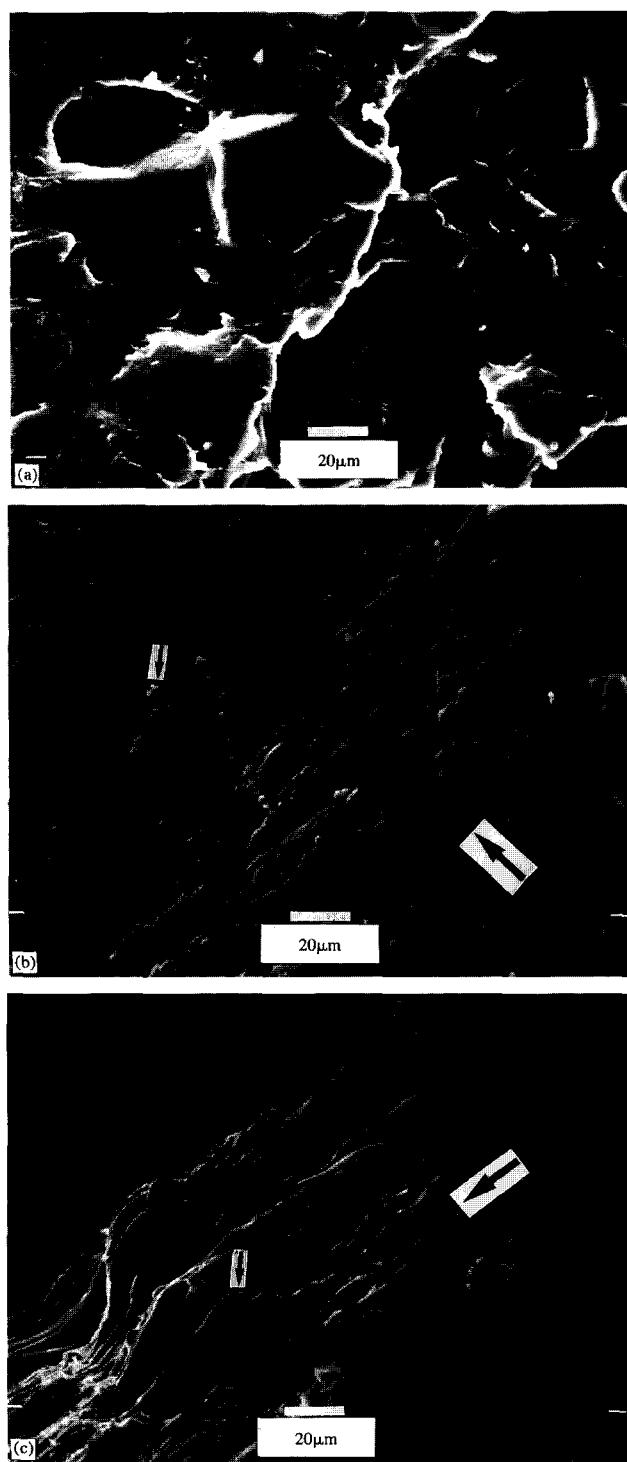


Figure 11 The SEM photographs of the same samples as in Figure 10. (a) Original sample (undrawn). (b) Prepared at 140°C and $CR = 8$ for the test of (\perp). (c) Same sample as in (b) for the test of (\parallel). The small arrows indicate the part in which the layer was elongated by the impact tests. The large arrows indicate the direction in which the hammer went through the sample

(pancake shaped) parallel to the film surface. Thus, the layer structure is seen in both crystal (b -axis orientation) and spherulite order. Figure 10 shows scanning electron microscopy (SEM) photographs of a surface fractured by the Izod impact tests. The large arrows on the photograph indicate the direction in which the hammer went through the sample. For the original undrawn

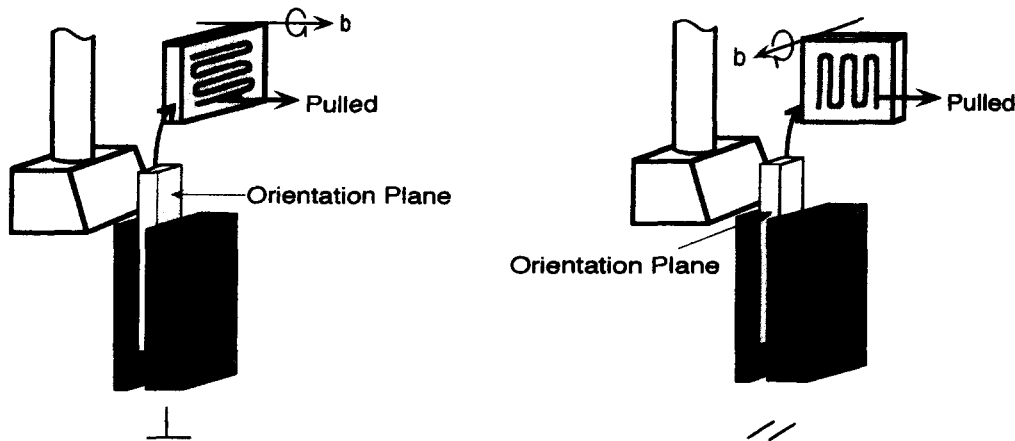


Figure 12 Schematic of crystal orientation in the forged samples for (\perp) and (\parallel) directions

sample, no layer structure is seen on fracture. The samples are broken into clusters on the scale of 10–50 μm diameter which is comparable to the average spherulite diameter of $\sim 35 \mu\text{m}$ (ref. 14). In the forged samples for both (\parallel) and (\perp), layered structures are seen in the fractured surface, stacked parallel to the sample surface. The layer thicknesses for (\parallel) and (\perp), judged by SEM, are 2–5 and 1–4 μm , respectively. Since the CR of this sample is 8, the spherulite is compressed to one-eighth of the original size, i.e. 1–6 μm . This is comparable to the layer thickness. This result indicates that a layer seems to be composed of deformed (pancake-shaped) spherulites.

The forged sample fractured into layers. Therefore, some of the impact energy is absorbed by the delamination of the layers. About 4 kgfcm cm^{-2} may be required to delaminate one layer as estimated for the (\parallel) direction. There are two factors to the mechanism of sample break of forged iPP: one is the delamination of each layer and another is the breaking of the layers themselves. The energy for the delamination of one layer (about 4 kgfcm cm^{-2} at $CR = 2.6$) must decrease with further draw (increasing CR) because of the orientation of crystal slip planes along the planar (\parallel) direction. On the other hand, the layer density, i.e. the number of layers per sample thickness (or cross-sectional area) increases with draw. For example, when CR is increased from 10 to 30 (three-fold increase), the layer density also increases three times. Further, the strength of each layer increases with draw because of the planar orientation of molecular chains. Opposing factors may provide a maximum of impact strength at an optimum CR. Chen *et al.* have reported¹⁷ that the impact toughness of laminated uniaxially drawn iPP goes through a pronounced maximum at the draw ratio of 10. This draw ratio corresponds to $CR = 100$. The optimum CR in which the maximum impact strength can thus be obtained might be higher than the CR used in this study ($CR < 36$).

Figure 11 emphasizes the difference of the fractured surfaces between (\parallel) and (\perp). As indicated by small arrows, the layers for (\parallel) and (\perp) are partially elongated along the hammer direction (indicated by a large arrow). The elongation at break for (\parallel) (Figure 11c), is larger than that for (\perp) (Figure 11b). This difference is closely related to the b -axis orientation of crystals in the layer,

i.e. the crystal $0k0$ planes orient parallel to the sample plane direction. The geometry of crystal orientation is shown in Figure 12. For (\perp), all lamellae or extended molecules must be pulled out of the layer since the hammer direction is perpendicular to the molecular axis or $0k0$ plane, leading to a break of layers at low elongation. For (\parallel), on the other hand, the molecules are pulled within the plane direction, since the hammer impacts parallel to the plane, leading to a high elongation at break. Major impact energy is absorbed by this mechanism. The fact that the impact strength for (\parallel) is about twice that for (\perp) (Figure 8) supports this energy absorption mechanism.

CONCLUSION

Anisotropy in microhardness of forged (planar oriented) iPP was observed between the directions perpendicular $H(\perp)$ and parallel $H(\parallel)$ to the film surface. The anisotropy, $H(\perp)/H(\parallel)$, increases with draw, which is mainly caused by the rapid decrease in $H(\parallel)$. The $H(\perp)/H(\parallel)$ for samples forged at 50°C (containing draw-generated smectic phase) is higher than that for samples forged at 140°C (composed of α -crystal only plus amorphous) at a comparable compression ratio. These are associated with the b -axis orientation of laterally disordered smectic phase normal to the (\parallel) direction (i.e. the disordered main slip $0k0$ plane lying in the (\parallel) direction).

The impact strength of forged samples is very different from the results of indentation tests. The effects of compression draw on the increase in impact strength, both parallel and perpendicular to the sample surface, are much greater than in microhardness indentation tests. There are two energy absorption mechanisms. One is delamination of the layers along the plane direction at break. The other is an elongation at break of the layers caused by the b -axis orientation of crystals within a layer. The former results in the increase in the impact strength for both (\parallel) and (\perp) directions. The latter is prominent for the (\parallel) direction, resulting in the strength for (\parallel) being about twice that for (\perp). The morphology-developed planar orientation lowers the hardness tested from the edge, but strongly enhances the impact property through the thickness and the plane directions.

REFERENCES

- 1 Ward, I. M. 'Mechanical Properties of Solid Polymers', Wiley-Interscience, New York, 1971, Ch. 10
- 2 Samuels, R. J. 'Structured Polymer Properties. The Identification, Interpretation, and Use of Polymer Structure', Wiley-Interscience, New York, 1974
- 3 Cao, B. and Sullivan, T. *SPE ANTEC Tech. Papers* **510**, 1995
- 4 Adams, G. C. *J. Polym. Sci. A-2* 1971, **9**, 1235
- 5 Kaito, A., Nakayama, K. and Kanetsuna, H. *J. Appl. Polym. Sci.* 1984 **29**, 2347
- 6 Minami, S. and Itoyama, K. *Am. Chem. Soc., Polym. Prepr.* 1985, **26**, 245
- 7 Sakai, Y. and Miyasaka, K. *Polymer* 1988, **29**, 1608
- 8 Sakai, Y. and Miyasaka, K. *Polymer* 1990, **31**, 5
- 9 Sakai, Y., Umetsu, K. and Miyasaka, K. *Polymer* 1993, **34**, 318
- 10 Gerrits, N. S. J. A., Young, R. J. and Lemstra, P. J. *Polymer* 1990, **31**, 231
- 11 Gerrits, N. S. J. A., Young, R. J. and Lemstra, P. J. *Polymer* 1991, **32**, 1770
- 12 Gerrits, N. S. J. A. and Young, R. J. *J. Polym. Sci. Part B: Polym. Phys.* 1991, **29**, 825
- 13 Osawa, S. and Porter, R. S. *Rept. Progr. Polym. Phys. Jpn* 1995, **38**, 431
- 14 Osawa, S., Porter, R. S. and Ito, M. *Polymer* 1994, **35**, 551
- 15 Watanabe, K., Kanda, T., Higashida, Y. and Kikuma, T., Nippon Steel Corp., personal communication
- 16 Austen, A. R. and Humphries, D. V. *SPE ANTEC Tech. Papers* **837**, 1982
- 17 Chen, H. J., Kortschot, M. I. and Leewis, K. G. *Polym. Eng. Sci.* 1994, **34**, 1016
- 18 Balta Calleja, F. J. *Adv. Polym. Sci.* 1985, **66**, 117
- 19 Balta Calleja, F. J., Martinez Salazar, J. and Asano, T. *J. Mater. Sci. Lett.* 1988, **7**, 165
- 20 Balta Calleja, F. J. and Kilian, H. G. *Colloid Polym. Sci.* 1985, **263**, 697
- 21 Martinez Salazar, J., Garcia, J. and Balta Calleja, F. J. *Polym. Commun.* 1985, **26**, 57
- 22 Fatou, J. G. *Eur. Polym. J.* 1971, **7**, 1057
- 23 Saraf, R. F. and Porter, R. S. *Polym. Eng. Sci.* 1988, **28**, 842
- 24 Osawa, S. and Porter, R. S. *Polymer* 1994, **35**, 540
- 25 Saraf, R. F. and Porter, R. S. *J. Rheol.* 1987, **31**, 59
- 26 Saraf, R. F. *Polymer* 1994, **35**, 1359
- 27 Osawa, S. and Porter, R. S. *Rept. Progr. Polym. Phys. Jpn* 1994, **37**, 379
- 28 Osawa, S. and Porter, R. S. *Polymer* 1994, **35**, 545
- 29 Brandrup, J. and Immergut, E. H. 'Polymer Handbook', 3rd edn, John Wiley, New York, 1989